Adsorption, Nucleation, and Growth of Cadmium on Tungsten Covered with Oxygen or Hydrogen

R. J. H. VOORHOEVE AND R. S. WAGNER

The effects of the adsorption of hydrogen and oxygen on the growth of cadmium from the vapor onto polycrystalline tungsten have been studied. We find that hydrogen does not affect the growth behavior in any way. Oxygen, on the other hand, drastically diminishes the chemisorption of cadmium on tungsten and inhibits growth. Appreciable supersaturation is needed to induce nucleation and growth on oxidized tungsten. Oxygen prevents epitaxial growth, leading instead to formation of small, irregularly oriented islands and of a few whiskers. Experimental results on the kinetics and topography of the deposition are compared with nucleation theory.

THE present state of affairs in the field of vapor-phase heterogeneous nucleation is characterized by the availability of much theoretical work, but there is still a paucity of experimental results.[1,2] Especially rare are experiments performed under "clean" conditions, and with proper characterization of the most important variables, *i.e.*, supersaturation, temperature, and surface coverage. Without such experiments it is difficult to test the existing theories and to properly assess the effects of adsorbed impurities.

Our earlier studies were concerned with the deposition of cadmium from the vapor onto clean, polycrystalline tungsten ribbons.[3] In that system, multilayer adsorption (3 to 4 monolayers) precedes growth of bulk cadmium. The heat of adsorption decreases, through five adsorption states, from 51 kcal per g-atom to a value close to the heat of sublimation of bulk cadmium, 26.6 kcal per g-atom. Growth of bulk cadmium occurs by the evolution of epitaxial islands and ridges from the adsorbed layer. No supersaturation is required for this process.

It is well-known that adsorption of contaminants, such as found in the atmosphere or in residual high vacuum, changes the characteristics of tungsten surfaces drastically. Not unexpectedly therefore, the adsorption of metals on tungsten is affected. For copper and beryllium the adsorption lifetime on oxygenated tungsten is appreciably higher than on clean tungsten. For iron and nickel, on the other hand, the lifetime decreases.[4,5]

Since adsorption of the condensing metal plays such a decisive role in the growth of cadmium on tungsten, it is expected that the nucleation and growth behavior will be strongly influenced by adsorption of contaminants. Indeed, preadsorption of nitrogen has been found to decrease the thermal accommodation coefficient, the lifetime and the adsorption energy, and to increase the critical supersaturation needed for growth.[6,7]

In the following, a study is presented of the effects of adsorbed hydrogen and oxygen on the adsorption, nucleation, growth, and epitaxy of cadmium on tungsten. The kinetics of the process were studied with a mass-spectrometric molecular-beam technique in ultra-high vacuum. The topography and morphology of the cadmium growth were observed by scanning electron microscopy.

R. J. H. VOORHOEVE and R. S. WAGNER are with Bell Telephone Laboratories, Inc., Murray Hill, N. J.

Manuscript submitted March 31, 1971.

1) EXPERIMENTAL

The apparatus, materials, and procedures used were the same as in our previous work.[3] Only a general outline will be given here.

In the center of an ultra-high vacuum chamber a 25 μm thick polycrystalline tungsten ribbon is mounted. This target is resistively heated and its temperature is measured and controlled by a tungsten/tungsten-rhenium thermocouple welded to the back. A resistively heated, enclosed, Knudsen cell provides a cadmium beam, which can be intercepted by a rotating shutter. In direct line of sight of the tungsten target, a quadrupole mass spectrometer is used to measure the intensity, and the temperature of the cadmium flux desorbing from the target. This instrument also provides analysis of the residual vacuum.

The base pressure of the apparatus is 2×10^{-10} torr. Oxygen or hydrogen may be admitted to the system through silver or silver-palladium diffusion tubes, respectively. Their purity was ascertained by *in situ* mass-spectrometric analysis. Helium is the main impurity and is possibly liberated from the Vac-Ion pump when it is pumping oxygen or hydrogen.

After going through preliminary cleaning, the tungsten target (99.95 pct purity) is placed in the chamber where it is further cleaned by heating in 10^{-7} torr oxygen to 2100°K to remove carbon, and subsequent heating to 2500°K in the residual vacuum (2 to 5×10^{-10} torr) to evaporate all oxides.[8,9]

The relation between the mass spectrometer detector current and the intensity of the cadmium flux desorbing from the target was calibrated by evaporating a thick cadmium deposit (500 to 1000 monolayers). Literature vapor pressure data[10] for bulk cadmium and the evaporation coefficient determined in Section 4 were used for the calibration. The calibration relation used is

$$I = 3.5 \times 10^{22} S_i \beta \frac{p_e}{\sqrt{MT}} \sqrt{\frac{T_{\text{ref}}}{T}} \qquad [1]$$

Here, I is the mass spectrometer current, S_i the calibration constant which is dependent on the sensitivity of the spectrometer and on the geometry of the system. p_e is the literature value for the cadmium vapor pressure at temperature T, M is the atomic weight of cadmium and T_{ref} is an arbitrary reference temperature. It was found that the evaporation constant β is 0.63 for clean[3] and hydrogen-covered tungsten and 0.90 for oxygenated tungsten.

After measuring S_i, the cadmium desorption rate from the target, v_0, can be found from the relation

$$v_0 = \frac{I}{S_i} \cdot \sqrt{\frac{T}{T_{ref}}} \qquad [2]$$

In this relation, the effects of thermal nonaccommodation are neglected. This is permissible because of the rather small deviation from complete accommodation (see below). Comparison of signals obtained from a cadmium beam of constant intensity "reflected" by clean and by oxidized tungsten also shows this to be a good approximation.

The thermal accommodation coefficient is defined by $(T_i - T_{ei})/(T_i - T_t)$, where T_i is the temperature of the incident beam, T_{ei} that of the beam coming from the target, and T_t is the temperature of the target. For cadmium impinging on oxygenated tungsten the accommodation coefficient is slightly less than unity. This is found by measuring the relation[6] between mass-spectrometer current and target temperature for an incident cadmium beam of constant intensity and temperature. It is also evident from the small step-response observed when the shutter is opened and the beam impinges on the oxygenated target. The magnitude of the step is about 2 to 3 pct of the impingement beam intensity.

2) HYDROGEN CONTAMINATION

The adsorption of hydrogen on tungsten has been studied in detail by flash desorption,[11,12] field emission,[13] and low-energy electron diffraction.[12] On polycrystalline tungsten, the heat of adsorption ranges from 35 kcal per mole for the bare substrate to 7 kcal per mole at monolayer coverage. At the low-coverage end, the adsorption is dissociative.[11] In line with this it was found that on (100) tungsten substrates the hydrogen forms two states, an atomic adsorption of 32.3 kcal per mole and a molecular adsorption of 26.3 kcal per mole. Both were inferred to be located in valleys between protruding tungsten atoms.[12]

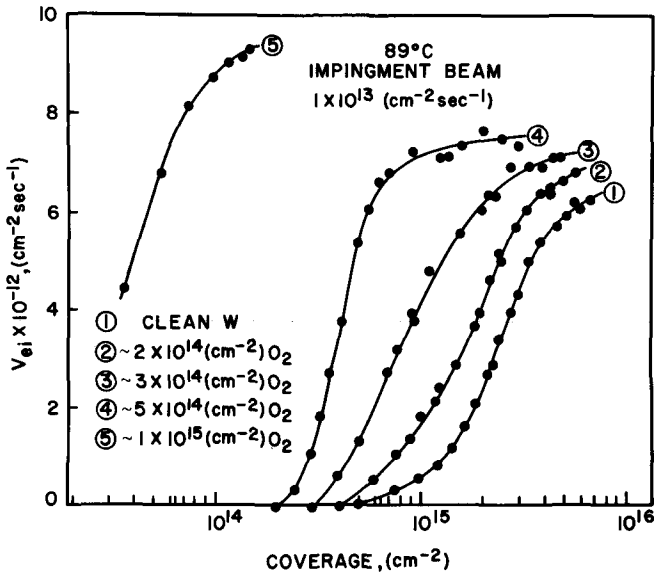

Fig. 1—Effect of oxygen exposure on the desorption transients at low supersaturation. Desorbed beam, v_{ei}, vs cadmium coverage.

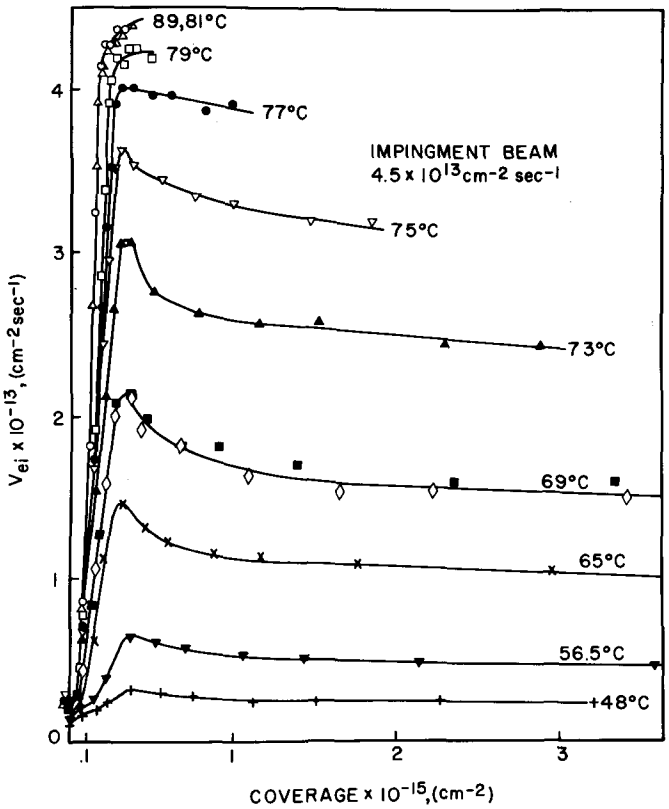

Fig. 2—Initial stages of adsorption, nucleation and growth. Tungsten temperatures are indicated near the curves. Critical cadmium adatom concentration 4×10^{14} cm^{-2}.

The effect of hydrogen on the adsorption and nucleation of cadmium was investigated by repeating several of the adsorption and growth experiments[3] in an ambient of 10^{-6} torr hydrogen. No changes were observed in either the adsorption or the growth kinetics. It is not possible to say whether cadmium replaces hydrogen on the surface, by virtue of its higher heat of adsorption, or whether hydrogen is incorporated into the cadmium adlayer. Even if the latter situation holds, no appreciable Cd-H interaction would be expected.[14] No effect of hydrogen on the desorption spectrum of cadmium from tungsten was found either.

3) ADSORPTION AND NUCLEATION OF CADMIUM ON OXYGENATED TUNGSTEN

Adsorption of oxygen on tungsten has been studied by many investigators.[9] Two different regimes can be distinguished. Low-temperature adsorption (<500°K) leads to the formation of an adlayer saturating at 1 to 1.5 monolayer of oxygen.[9,15] In high-temperature adsorption, the surface tungsten layer is reconstructed with formation of an oxide-surface compound. At 750°C, faceting of (100), (112), and (111) faces was

observed, leading to {110} orientations.[15,16] The heat of adsorption of oxygen[9,17,18] is 100 to 140 kcal per g-atom, much higher than that for cadmium, which varies from 51 to 27 kcal per g-atom. It is not expected that CdO can be formed from the adsorbed oxygen, as the heat of formation of the oxide is much lower than that of any tungsten oxides.[19] In any case, CdO was not detected by the mass spectrometer.

Both high-temperature and room-temperature adsorption of oxygen were employed in the present work, and the effects on the adsorption and nucleation of cadmium were studied.

Effect of Oxygen on Adsorption of Cadmium

After the usual cleaning of the tungsten foil and flashing to 2200°C in less than 5×10^{-10} torr residual gas, the foil was exposed to 9×10^{-10} torr oxygen at room temperature. This causes no reconstruction of the tungsten surface.[9] After the required exposure time, the oxygen flow through the silver diffusion tube was turned off and the pressure decreased rapidly to 2×10^{-10} torr. Various coverages with oxygen could be obtained by varying the exposure time. Following this preadsorption of oxygen, the temperature of the target was raised slightly, and a cadmium beam of intensity v_i was allowed to impinge on the tungsten target by opening the shutter. A cadmium "desorption transient" was measured, showing the rate of desorption of cadmium (v_{ei}) as a function of the time elapsed since opening the shutter. The cadmium coverage at any time t is given by

$$\sigma = \int_0^t (v_i - v_{ei})dt \qquad [3]$$

In Fig. 1, a number of desorption transients have been plotted as v_{ei} vs coverage, σ, for different values of the preadsorption exposure of oxygen. One sees that, at 89°C, a clean tungsten substrate (curve No. 1) adsorbs about 7×10^{14} cm^{-2} cadmium before a measurable cadmium desorption rate is obtained. The growth rate is given by the difference between the in-

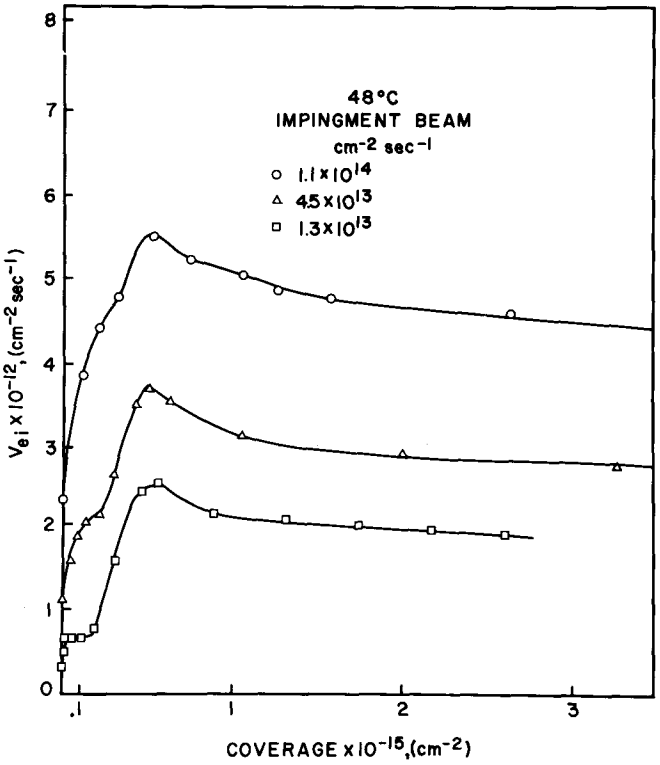

Fig. 3—Nucleation and growth; effect of incident beam intensity on the desorption rate at a substrate temperature of 48°C.

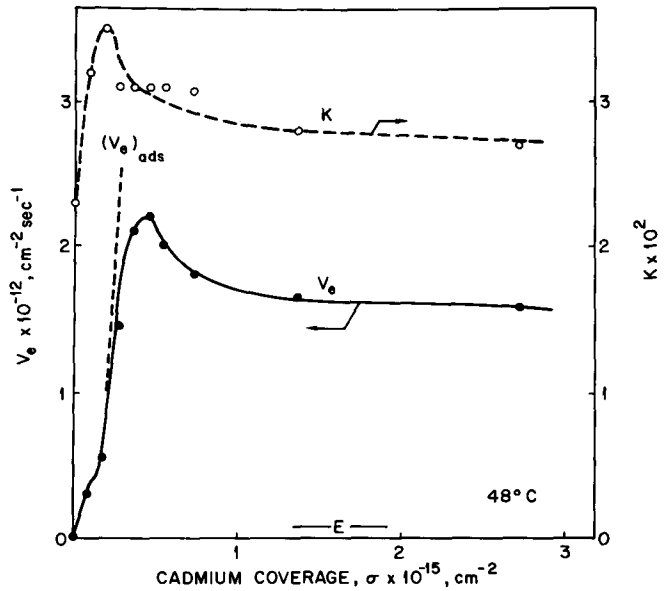

Fig. 4—Equilibrium evaporation rate v_e and evaporation coefficient K, derived from data of Fig. 3 by Eq. [4].

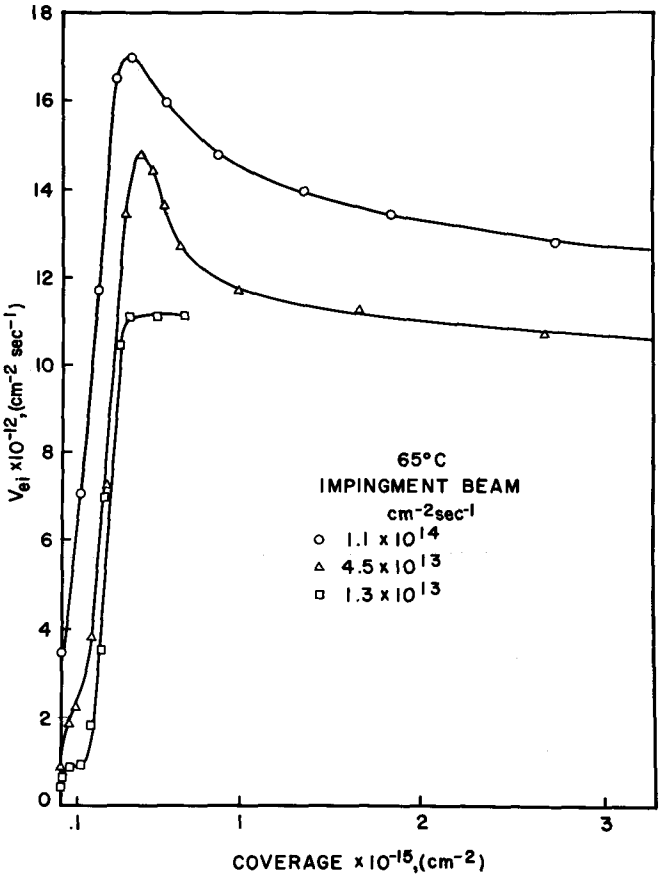

Fig. 5—Nucleation and growth, effect of incident beam intensity on the desorption rate at substrate temperature of 65°C.

cident beam intensity, 10^{13} cm^{-2} sec^{-1}, and the desorption rate depicted in Fig. 1. The amount of tightly-bound cadmium diminishes rapidly with increasing oxygen-coverage. With 5×10^{14} cm^{-2} oxygen on the surface, only about 2×10^{14} cm^{-2} cadmium is tightly bound (curve No. 4). The cadmium growth rate ($v_i - v_{ei}$), which, for clean tungsten, is about 3×10^{12} cm^{-2} sec^{-1} at the end of the experiment (curve No. 1), also diminishes, and 10^{15} cm^{-2} oxygen suppresses growth almost completely (the desorption rate rises to approximately 95 pct of the incident beam at a cadmium coverage just over 10^{14} cm^{-2}).

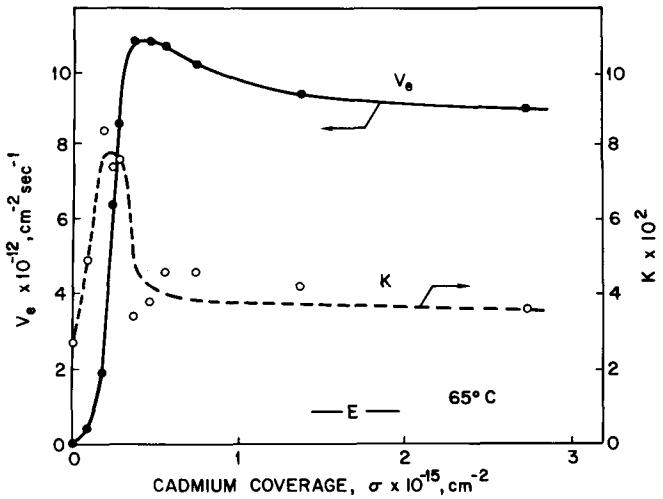

Fig. 6—Equilibrium evaporation rate v_e and evaporation constant K, derived from data of Fig. 5 by Eq. [4].

All further experiments were done with a tungsten surface oxidized by heating in 10^{-8} torr oxygen at 1000°C, and then slowly cooled to room temperature in the same ambient. The surface consisted then of a reconstructed oxide layer.[15,16] In Fig. 2, a number of nucleation experiments are plotted as v_{ei} vs σ. They are done in the same way as desorption transients, but at higher supersaturations. The supersaturation

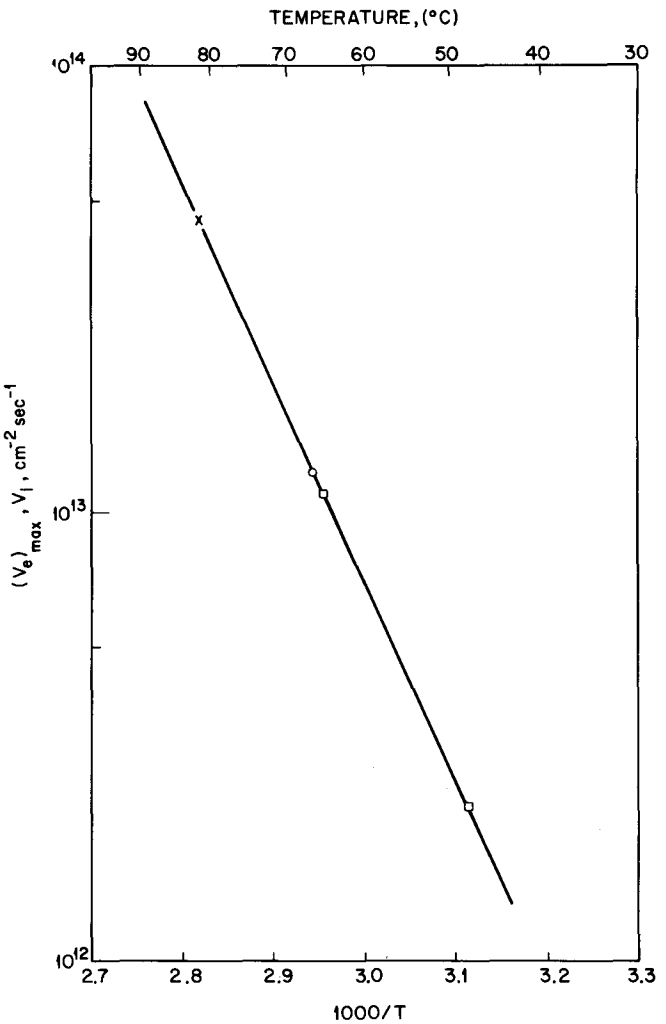

Fig. 7—Critical incident beam intensity and equilibrium evaporation rate vs reciprocal temperature. × obtained from Fig. 2 by extrapolation to $v_i - (v_{ei})_{max} = 0$, ○ direct measurement performed by cooling the substrate at constant incident beam intensity, □ $(v_e)_{max}$ from Figs. 4 and 6.

Table I. Thermodynamic Parameters of Cadmium on Oxidized Tungsten

Cadmium Coverage, cm^{-2}	Enthalpy Change, Solid to Gas, ΔH, kcal/gm-at.	Gibbs Free Energy Change, Solid to Gas, $\Delta G_{336°K}$, kcal/gm-at.	Species on the Surface
1.8×10^{14}	18.5 ± 1	15.98	monomers
4.0×10^{14}	20.8 ± 0.5	15.59	critical nuclei
2.5×10^{15}	21.5 ± 0.5	15.74	nuclei
5.0×10^{17}	26.7 ± 0.5	17.28	islands, coalesced

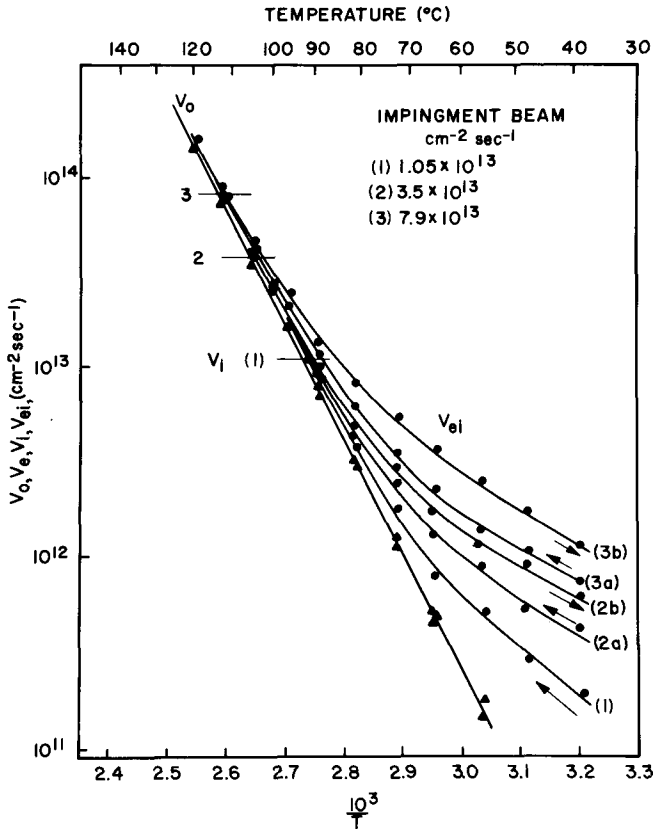

Fig. 8—Evaporation and condensation on a thick cadmium deposit (~500 monolayers). Heating curves 1, 2*a*, and 3*a* obtained after 5 to 10 min equilibration at room temperature, with the beam on. Cooling curves 2*b* and 3*b* show the hysteresis. Langmuir evaporation rate given by v_0. Heating and cooling rates 1°K per sec.

is defined as the ratio of the incident beam intensity to the equilibrium evaporation rate of bulk cadmium, $v_i/(v_e)$ bulk.

Upon opening the cadmium beam shutter, a step response in the mass-spectrometer signal indicates incomplete thermal accommodation of cadmium. As the heat of adsorption is appreciable (see below), it must be assumed that it is only a small fraction of the surface which elastically reflects about 2 pct of the incident beam. This percentage increases slightly with rising temperature. The effect is visible in Fig. 2 in that the v_{ei} curves do not start at $v_{ei} = 0$ for $\sigma = 0$. The step response was observed at the instrumental time constant of 0.5 sec.

The v_{ei} curves have an initial flat portion, similar to the case of nitrogen-contaminated tungsten.[6,7] This is due to a rather tightly-bound state in which about 1 to 2×10^{14} atoms per sq cm may be adsorbed.

Evidence for a Nucleation Barrier

In the temperature range of 48° to 77°C, for which the impingement beam employed in Fig. 2 corresponds to supersaturations from 700 to 15, a maximum is found in v_{ei} at 4×10^{14} cm^{-2} cadmium coverage. This maximum, equivalent to a minimum in the growth rate, shows the presence of a nucleation barrier. The coverage at which it occurs is therefore the critical adatom concentration for nucleation. This appears to be independent of temperature. Its value, however, seems rather high in the light of the statistical theory of heterogeneous nucleation.

At insufficient supersaturation, *e.g.*, 89°C in Fig. 2, a coverage close to this critical adcoverage is established but no further growth occurs.

A more detailed examination of adsorption and nucleation is possible using experiments shown in Figs. 3 and 5. In this series, nucleation experiments were done at constant temperature for three beam intensities v_i. It is evident that the v_{ei} curves for different v_i do not coincide, indicating nonequilibrium between the gas phase and the adlayer. Part of this is due to the incomplete thermal accommodation, and part might be due to the presence of a loosely-bound precursor state. If equilibrium existed, the desorption rate would be a function of coverage and temperature only. With a precursor state present, the evaporation rate would be a function of the fraction of the cadmium present in that state.

Analysis of Nucleation Curves v_{ei} vs σ

The sets of curves in Figs. 3 and 5 have been analyzed by plotting the desorption rate v_{ei} vs the incident beam intensity v_i for constant coverage σ. A relation is found which is rather well approximated by

$$v_{ei} = v_e + K(v_i - v_e) \qquad [4]$$

Under experimental conditions where there is no net growth or evaporation, meaning $v_i = v_{ei}$, the "equilibrium" desorption rate, v_e is obtained. At high coverage v_e becomes equivalent to the equilibrium bulk vapor pressure of cadmium, irrespective of the nature of the substrate. The desorption constant, K, includes the effect of thermal nonaccommodation. Values of K and v_e derived with Eq. [4] are plotted in Figs. 4 and 6 as a function of the cadmium coverage. Values of v_e are more reliable than those of K, especially near the critical coverage of about 4×10^{14} cm^{-2} where Eq. [4] is only a fair approximation.

Focusing attention on the v_e curves, it is observed that the maximum in the equilibrium desorption rate, at the critical coverage, corresponds to a peak in the free energy of formation of the cadmium nuclei. We thus measure in a rather direct way the vapor pressure of the critical nuclei.

The initial parts of the v_e curves, up to the maximum, give the vapor pressure of an adpopulation which at low coverage consists almost exclusively of monomers. Without clustering, that is without Cd-Cd

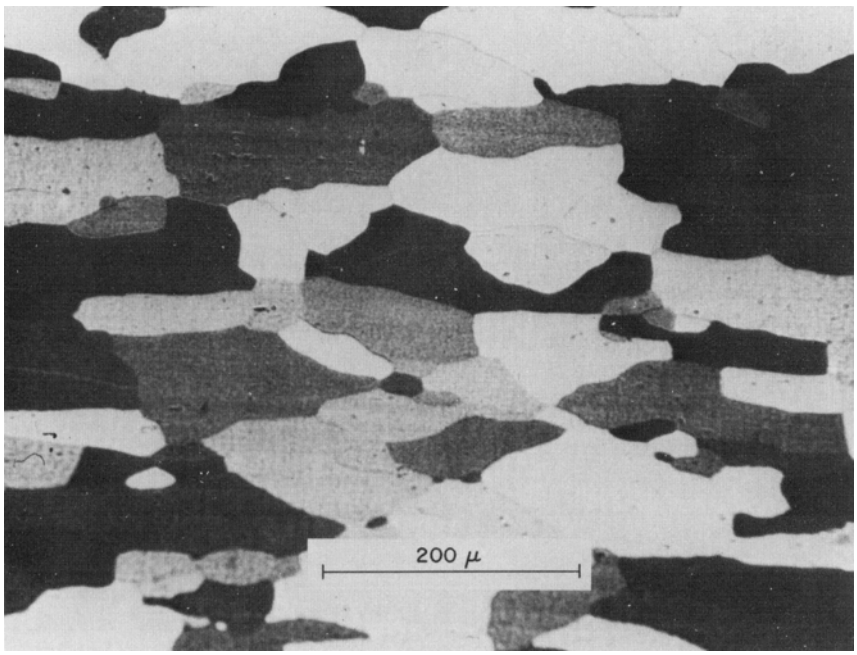

Fig. 9—Light micrograph of thin cadmium deposit, average coverage about 70° monolayers, deposited at 48°C, beam intensity 3×10^{13} cm^{-2} sec^{-1}.

attraction, the coverage would saturate, giving a v_e curve as roughly indicated by $(v_e)_{ads}$ in Fig. 4. The inflection point in the rising part of the v_e curve, at about 2×10^{14} cm^{-2} coverage, may perhaps be regarded as the onset of noticeable embryo formation or clustering. Up to the maximum, the v_e curve represents the condition of equilibrium between the deposit and the gas phase, in the absence of bulk cadmium (conditional or metastable equilibrium).

Beyond the maximum in v_e, this quantity gives the minimum incident rate necessary for growth. However, a deposit held at a particular $\{T, \sigma, v_e\}$ combination, represented by a point on the v_e curve, is not in equilibrium with the gas phase. It is easily verified that any infinitesimal difference between incident beam and evaporation flux will tend to increase, removing the system from the particular point on the curve.

The heat of desorption of monomers and the heat of evaporation of nuclei were determined from v_e curves for 48° and 65°C, Table I, with the formula $\Delta H(\sigma) = R[\Delta(\ln v_e)/\Delta(1/T)]_\sigma$. An indication of the accuracy was derived from the scatter of v_{ei} measurements. At a cadmium coverage of 1.8×10^{14} cm^{-2}, where clustering is probably still rather unimportant, the heat of adsorption of monomers is found. It is 18.5 kcal per g-atom, compared with 26.7 kcal per g-atom for the heat of sublimation of bulk cadmium.[10,19] At the critical adatom-concentration, 4.0×10^{14} cm^{-2}, the heat of evaporation is about 20.8 kcal per g-atom, the difference of 2 kcal per g-atom reflecting the cadmium-cadmium interaction in the cluster. Of course, the average cadmium-substrate interaction for the atoms in the cluster may well be smaller than the heat of adsorption of 18.5 kcal per g-atom, and 2 kcal per g-atom is therefore a minimum value for the Cd-Cd interaction.*

*The binding energy for a gaseous cadmium dimer was found to be 2.0 kcal per mole.[20,21]

Critical Supersaturation

The critical supersaturation for nucleation of cadmium on oxygenated tungsten was determined in three ways. The first one is to let a cadmium beam impinge on the surface, while slowly cooling the tungsten from about 400°C to room temperature. Nucleation is manifest by a rather sharp drop in the intensity of the desorbed cadmium flux.[6,7] Another way is to determine, from a plot such as Fig. 2, at what temperature the minimum growth rate (given by $v_i - v_{ei}$ at the v_{ei} maximum) becomes zero. It is also possible to calculate the critical supersaturation from the maximum in v_e, Figs. 4 and 6, as it must be equal to the ratio $(v_e)_{max}/(v_e)_{bulk}$.

Values for the critical supersaturation obtained from these three methods are shown in Fig. 7 as a function of temperature. The close agreement of the direct measurement (at 67°C) with the value calculated from the v_e maximum (at 65°C) supports the interpretation that $(v_e)_{max}$ is equivalent to the equilibrium vapor pressure of the critical nuclei.† The data can be represented by the formula

$$\log v_i^* = 26.5 - \frac{20{,}800}{2.3\,RT} \qquad [5]$$

Here, v_i^* is the critical impingement rate and RT is in cal per mole.

†Data we recently obtained for the nucleation of cadmium on single crystal germanium also support this interpretation.

4) GROWTH AND STRUCTURE OF THICK CADMIUM LAYERS ON OXIDIZED TUNGSTEN

The growth and structure of thick cadmium layers (≥50 monolayers) have been studied by kinetic meas-

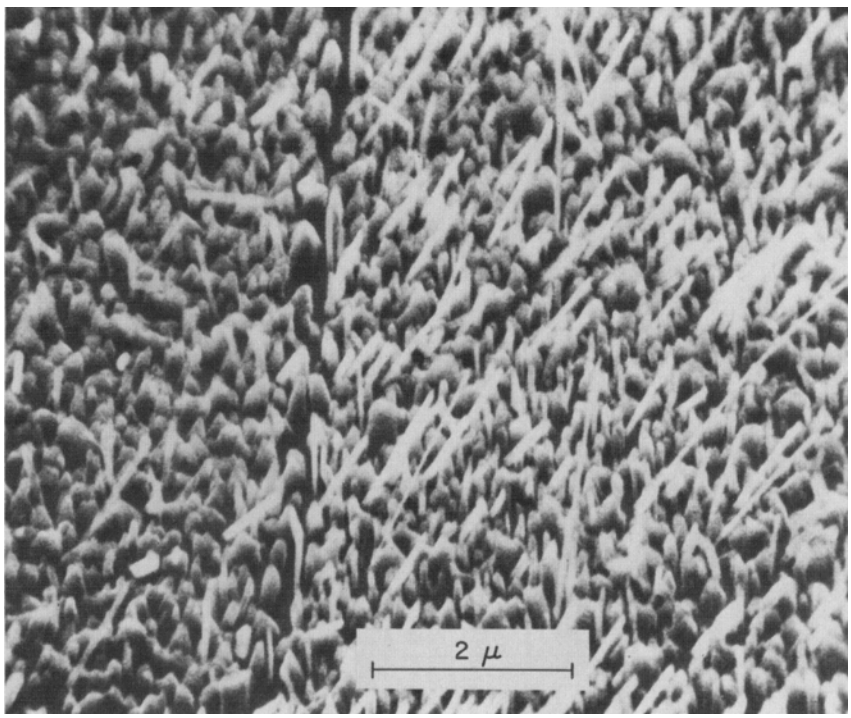

Fig. 10—Scanning electron micrograph of two tungsten grains with cadmium deposit of 70 monolayers; see subscript Fig. 9.

urements, scanning electron microscopy, optical microscopy, and by electron microscopy of replicas.

Evaporation and Condensation

The sublimation rate of a cadmium layer of 500 monolayers thick was measured as a function of temperature and incident beam intensity. Results plotted in Fig. 8 show that there is appreciable hysteresis in v_{ei} when the tungsten is cycled at a rate of 1°K per sec from low to high temperature with the beam on (see curves $2a$ and $2b$, or $3a$ and $3b$). This indicates that the structure of the deposit is a function of the temperature. It takes in the order of 10 to 100 sec to establish the steady-state surface configurations. After a stay at high temperature, the deposit presumably has a smoother surface and the number of growth sites has diminished.

At the temperatures where the incident beam intensity and the sublimation rate become equal ($v_i = v_{ei}$) there is equilibrium between the gas phase and the solid. The hysteresis effect is absent there. The locus of the points $v_i = v_{ei}$ in Fig. 8 is therefore the equilibrium vapor pressure curve, v_e. It is parallel to, but slightly higher than the Langmuir evaporation curve, v_0. The slope gives a heat of sublimation of 27.7 kcal per g-atom, in good agreement with an accepted literature value of 26.7 kcal per g-atom.[10] The evaporation coefficient, β, is given by

$$\beta = \frac{v_0}{v_e} = 0.90 \qquad [6]$$

This is to be compared with $\beta = 0.63$ for epitaxially grown cadmium on clean tungsten[3] and a value of $\beta = 1.0$ for bulk polycrystalline cadmium.[22] The higher value in the present work is in line with the rather fine-grained structure of the cadmium films on oxidized tungsten, as compared to the smooth and highly-oriented epitaxial cadmium films.

Comparing the v_{ei} curves of Fig. 8 with similar curves for cadmium on clean tungsten, Fig. 11 in Ref. 3, shows that v_{ei} is generally lower in the present case, as would be expected for a highly imperfect deposit.

Morphology of Cadmium Films

The morphology of the present films is illustrated by Figs. 10 through 16. In thin films, about 70 monolayers thick, optical micrographs, Fig. 9, show that the cadmium decorates the grain-structure of the tungsten substrate. However, little variation is detected in the fine structure of the cadmium deposit on the various tungsten grains. This observation is confirmed by scanning electron micrographs, Fig. 10. There are some exceptional grains, however, which do show a different structure, with epitaxial alignment of the cadmium crystals, Fig. 11.

Thick cadmium deposits (500 monolayers) show under the light microscope hardly any morphological variation from one tungsten grain to the other, Fig. 12. The contrast with deposits of similar thickness on clean tungsten is striking, see Fig. 9 of Ref. 3. Scanning electron micrographs, Fig. 13, show that many of the larger crystals in the deposit have the hexagonal morphology of bulk cadmium. Some appear to be twinned. The bimodal size-distribution of the islands in Fig. 13 cannot be explained by nucleation at two different supersaturations, since constant deposition conditions were employed. The larger islands may have formed by coalescence and Ostwald ripening.

In the fringe-area of the beam spot on the tungsten target, the small crystallites of Fig. 14 were observed. They show a cadmium-substrate "contact

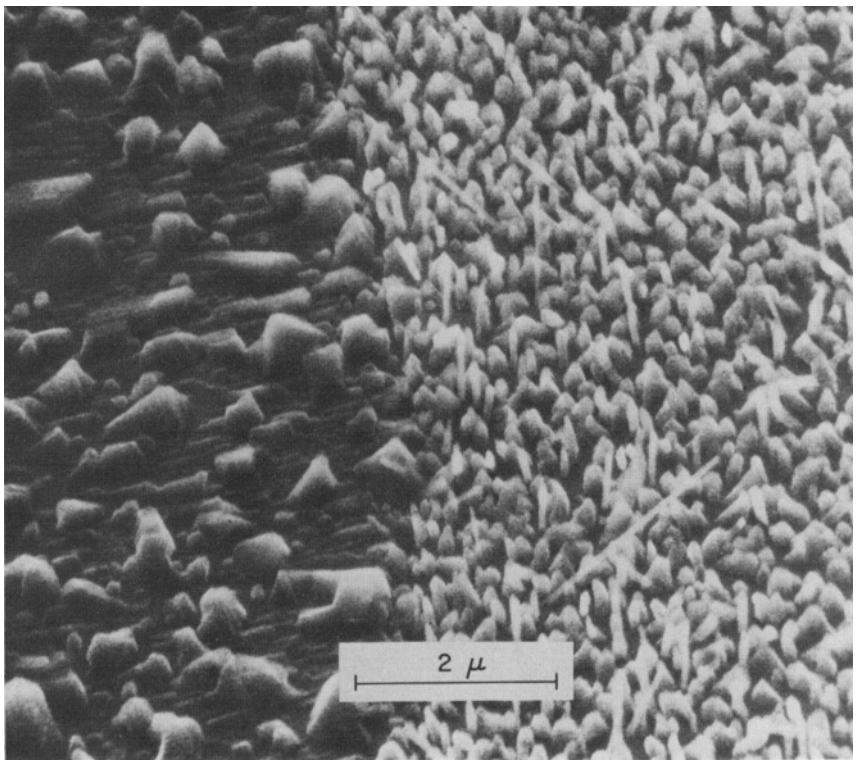

Fig. 11—Scanning electron micrograph of cadmium deposit of 70 monolayers; see subscript Fig. 9. At left one of the rare grains with preferred orientation of the cadmium.

angle'' of about 80 deg. Of course this is largely determined by the crystallography and is not necessarily equal to the contact angle θ resulting from the balance of surface tensions. However, in view of the value found and of the further characteristics of the deposit (*e.g.*, the presence of whiskers) the angle θ must be rather high too. Since the grain boundaries of the tungsten substrate have acquired a *V*-shaped cross-section through thermal etching, theory[23,24] would predict a particularly favorable situation for nucleation at the boundaries for $\theta \sim 90$ deg. However, on all the micrographs obtained, Figs. 10, 11, and 14, decoration of the grain boundaries is absent. Therefore it must be assumed that $\theta > 90$ deg.

Whiskers

Many whiskers were found in both thin and thick cadmium films on oxidized tungsten. On clean tungsten they had been completely absent.[3] The whiskers are quite numerous on some grains, completely absent on others, Figs. 10 and 11. Sometimes they are concentrated on a grain boundary, Fig. 15. They typically have a length/diameter ratio of about 50. In making a replica of one sample, many whiskers stuck to the replica and were stripped off. Electron diffraction confirmed that they are cadmium with the hcp crystal structure.

The mechanism of formation of the whiskers is not clear. They are formed during cadmium deposition and did not grow during storage, as stress-induced whiskers would.[25] They do not seem to grow through a VLS mechanism[26] either. On the other hand, the orientation of the whiskers with respect to the substrate is not random; neighboring whiskers are often parallel, Figs. 10, 15, and 16. This indicates some influence of the orientation of the tungsten grain on their growth direction.

In view of the limited amount of material present in the form of whiskers, no appreciable effect on the overall growth kinetics of the films is expected.

5) COMPARISON WITH HETEROGENEOUS NUCLEATION THEORY

Heterogeneous nucleation of a vapor on a surface acting as nucleation ''catalyst'' is classically de-

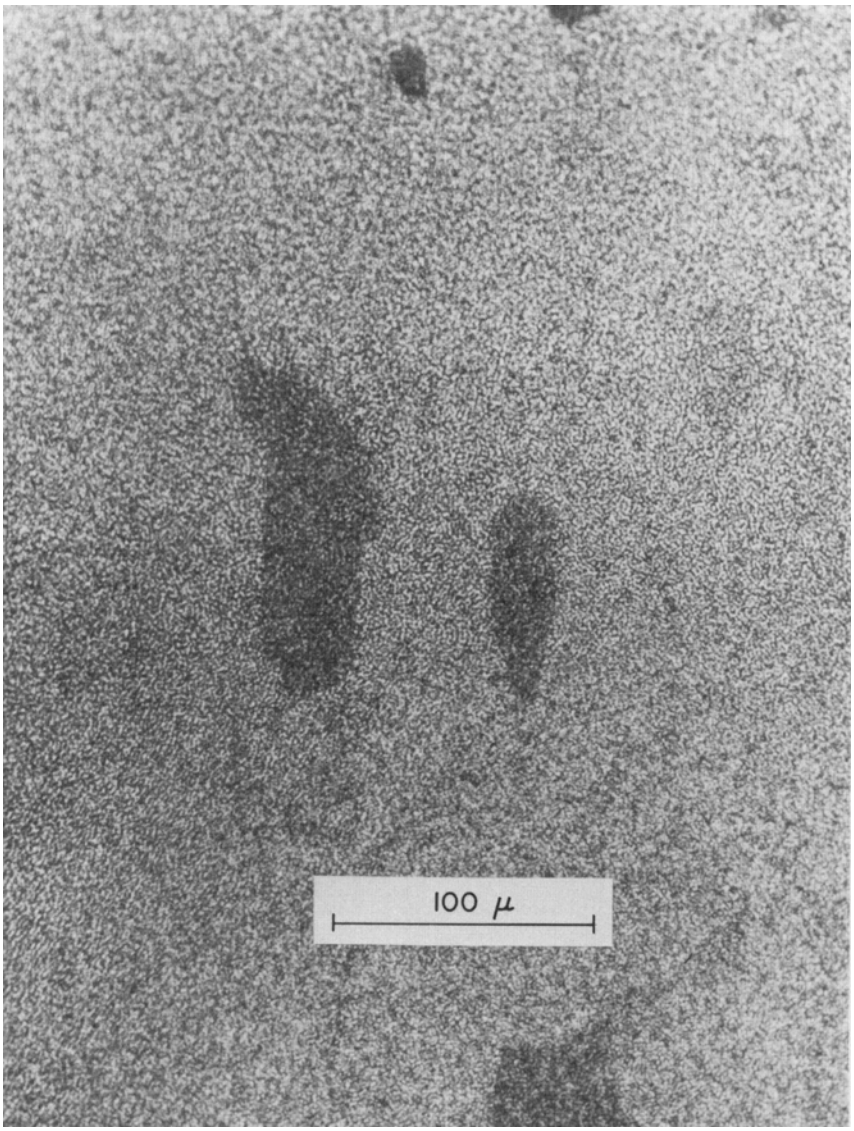

Fig. 12—Light micrograph of thick cadmium deposit, average coverage about 500 monolayers, deposited at 48°C, beam intensity 7×10^{13} cm^{-2} sec^{-1}.

scribed as a process involving adsorption of vapor atoms onto the surface to form a dilute adlayer, in which nuclei form by surface migration and ensuing statistical variations of the local concentration.[27] It was recognized by Gibbs[28] that such systems pass through a free energy maximum as the size of these nuclei is increased. This maximum has been associated with the existence of a critical nucleus, which would have equal probabilities of decay or further growth.[29,30]

Critical Adatom Concentration

In the classic nucleation theory, the total adatom concentration is usually assumed to be very small compared to the monolayer. It has to be, since the number of pairs, triplets, and so forth, rises rapidly with increasing coverage of the surface. High critical adatom concentrations would have as a corollary extremely large critical nuclei or, in other words, very small energies of attraction between the adatoms. Take, for instance, atoms with a pair interaction of $-2kT$ adsorbed on a square lattice. This adlayer becomes unstable with respect to condensation to dense clusters at a relative coverage $n_1^*/N \simeq 2 \times 10^{-2}$ (Ref. 31). N is here the number of sites per unit area, n_1^* is the number density of single atoms at nucleation.

In the case of the condensation of metals, pair interaction energies are much larger than kT under the usual experimental conditions, and critical adpopulations $n_1^*/N \ll 10^{-2}$ would thus be expected. However, for silver on tungsten a critical adpopulation of $n_1^*/N \sim 0.2$ was found, and the radius of the critical nucleus was calculated to be 1.5Å (Refs. 32 and 33). In the present case of cadmium on oxygenated tungsten the observed critical adpopulation is 4.0×10^{14} cm^{-2} or $n_1^*/N \simeq 0.4$. It is evident that these high adpopulations are not consistent with cluster formation by statistical distribution of the adatoms over the surface. The discrepancy can be explained by assuming that the adatoms fill tight-binding sites and are not participating in cluster formation because the interatomic distance in the cluster, which should be close to that in the bulk metal, is too different from the distance between the surface sites. This would lead to an average substrate-adatom interaction which is appreciably lower for the cluster than for single atoms, resulting in low or even vanishing net interaction energies. The total coverage in such a case is of less importance than the excess population after saturation of the adsorption sites.

The Critical Supersaturation

The explanation and prediction of the critical supersaturation and its temperature dependence have been treated both as an equilibrium problem[34,35] and as a kinetic problem.[27,29,36,37] In the equilibrium treatment, the conditions are calculated for the phase transformation of the adsorbed lattice gas into a condensed phase. Neglecting the effect of attraction between adatoms on the entropy, Fowler and Guggenheim derived the following formula for the phase transformation:

$$v_i^* = \frac{2\pi m \nu^3}{kT} \exp\left[-(2\Delta h_0 - z\epsilon_2)/2kT\right] \qquad [7]$$

where v_i^* is the critical intensity of the impingement beam at condensation temperature T, ν is the geometric mean of the frequencies for the three directions of vibration in the localized monolayer, z is the coordination number of the lattice, and Δh_0 and ϵ_2 are the atomic heat of adsorption and the pair interaction energy, respectively. The atomic mass is denoted by m, the Boltzmann constant by k. The relation should give a straight line when log v_i^* is plotted vs $1/T$, and this is in agreement with the experimental results,

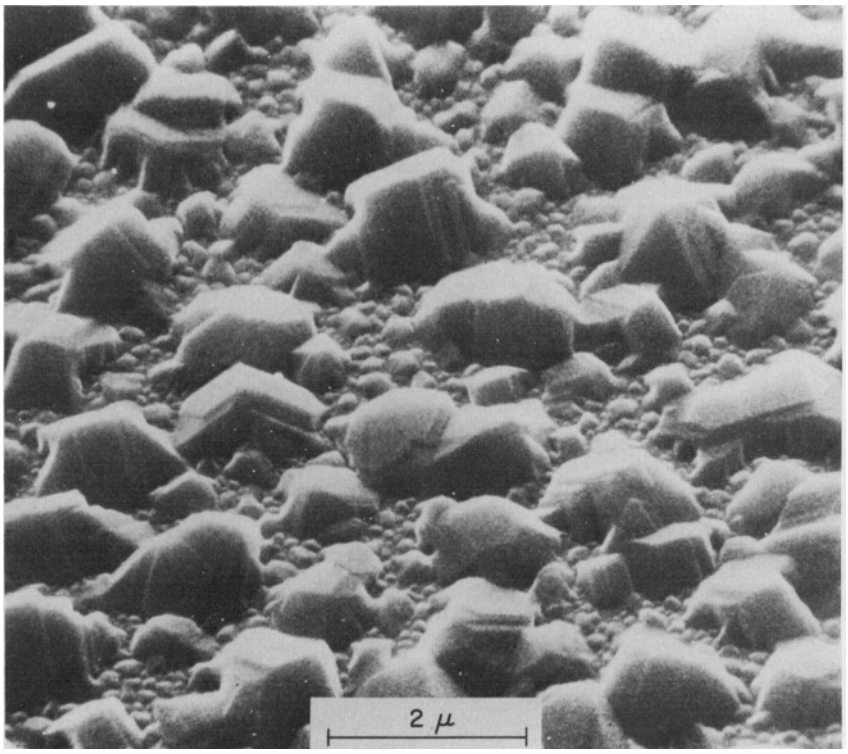

Fig. 13—Scanning electron micrograph of cadmium deposit of 500 monolayers; see subscript Fig. 12.

Fig. 7 and Eq. [5]. However, the preexponential factor predicted by Eq. [7] is $10^{28.6}$ cm^{-2} sec^{-1}, a factor 125 higher than the $10^{26.5}$ cm^{-2} sec^{-1} found experimentally. (A frequency $\nu = 10^{12}$ sec^{-1} was used in Eq. [7]). The formula also predicts too high preexponentials for the condensation in other systems.[34,38]

In a similar treatment of the problem,[35] the entropy of the adsorbed atoms is represented by that of three translational degrees of freedom, leading to the expression:†

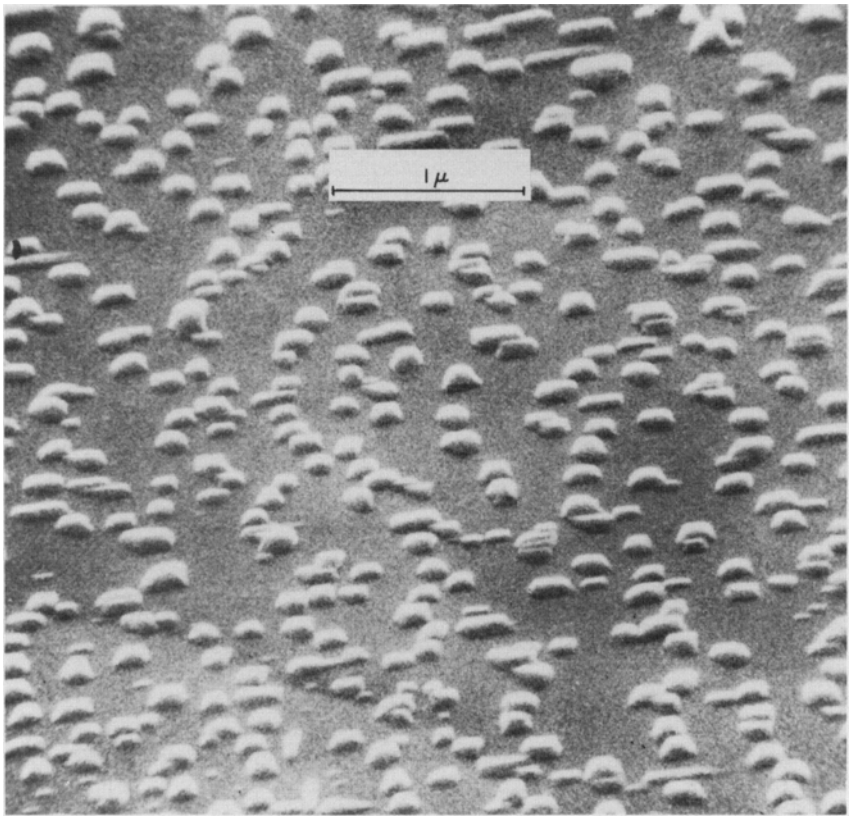

Fig. 14—Scanning electron micrograph of fringe area of cadmium deposit. A tungsten grain boundary is visible in the lower left-hand corner.

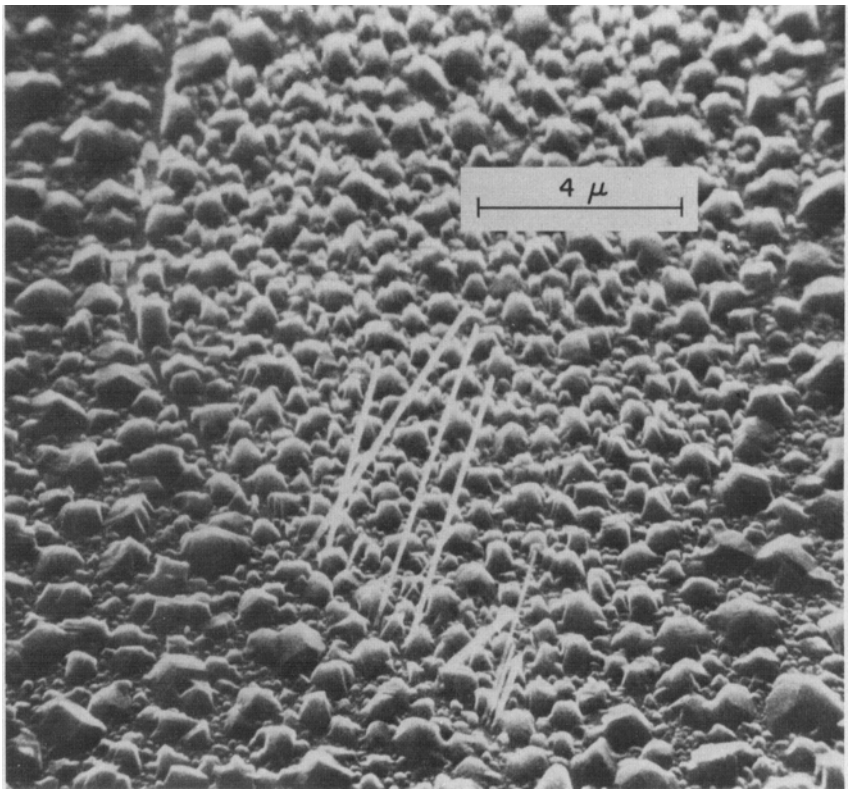

Fig. 15—Cadmium whiskers on a tungsten grain boundary. Scanning electron micrograph of a deposit of 500 monolayers average thickness; see subscript Fig. 12.

*The expression given by Walton has been changed in two ways: it is written to give ν_i^* in incident rates rather than pressures by dividing by $(2\pi mkT)^{1/2}$, and ν has been placed in the denominator rather than in the numerator, which is a correction of an obvious oversight. Eq. [8] becomes identical to Eq. [7] when the entropy of the adsorbed atoms is represented by three harmonic oscillations rather than three translational degrees of freedom, and $\Omega_0 = 1$.

$$\nu_i^* = \left(\frac{kT}{2\pi m}\right)^{1/2} \frac{\Omega_0}{v} \exp\left[-(2\Delta h_0 - z\epsilon_2)/2kT\right] \qquad [8]$$

Here, Ω_0 stands for the contribution of the ground state of the atom to the electronic partition function, and v is the volume associated with one surface site. This model is clearly overestimating the entropy of the adsorbed phase, and it is therefore yielding preexponential factors that are much too low. One calculates the factor to be $10^{19.3}$ cm^{-2} sec^{-1} from Eq. [8], as compared to the experimental $10^{26.5}$ cm^{-2} sec^{-1}.

It should be noted that in the derivation of Eqs. [7] and [8] the total interaction energy of the clusters has been assumed to be proportional to the number of pairs, which is a rather poor assumption, especially for the metals of group IIB (Refs. 39 and 40).

The capillarity theory of critical nucleation rates[29,36,37] uses contact angles and surface energies determined in systems of macroscopic size to express the free energy of the critical cluster. The following equation, based on the Gibbs-Thomson relationship, is found:[37,41]

$$\left(\frac{kT}{V} \ln \frac{p^*}{p_e}\right)^{-2} = \frac{3}{16\pi\sigma^3\Phi(\theta)} \{kT(\ln C + 2 \ln p^*) + 2\Delta G^*_{des} - \Delta G^*_{sm}\} \qquad [9]$$

Herein,

$$C = \frac{a \sin\theta \ln(p^*/p_e)}{8\pi m} \left\{\frac{1}{3}\Phi(\theta)\sigma kT\right\}^{-1/2} \qquad [10]$$

This relation has been evaluated for the present experimental values for p^* and T, from Fig. 7, and a contact angle $\theta = 90$ deg (but see Section 4) which yields $\Phi(\theta) = 0.50$ (Ref. 41). ΔG^*_{des} was calculated from the experimental heat of adsorption $\Delta H_0 = 18.5$ kcal per g-atom while neglecting the translational degrees of freedom of the atoms in the adlayer. The barrier for surface migration ΔG^*_{des} was neglected. For the lattice constant, $a = 4 \times 10^{-8}$ cm was used, and for the surface energy, $\sigma = 700$ erg per sq cm (Ref. 42). V is the atomic volume of bulk cadmium, k, T, and m have the usual meanings, and $\nu = 10^{12}$ sec^{-1} is the jump frequency on the surface.

The values for $\ln(p^*/p_e)$ calculated with Eq. [9] are a factor 10 larger than the experimental results, resulting in values for p^* which are a factor 10^{10} to 10^{13} too high. This large discrepancy cannot be due to the assumptions made for θ, ΔG^*_{des} and ΔG^*_{sm}, but seems to result largely from the use of a bulk value for σ. Agreement can be obtained with $\sigma = 160$ erg cm^{-2}. However, the basis of the capillarity theory is the use of bulk values for the energy parameters. Reduction of σ to an adjustable parameter would make the value of the theory rather questionable.

6) SUMMARY AND CONCLUSIONS

The effect of hydrogen preadsorption and a hydrogen ambient on the condensation of cadmium vapor on polycrystalline tungsten is negligible. This is probably due to the rather weak affinity of hydrogen for either tungsten or cadmium.

Oxygen, on the other hand, being strongly chemisorbed on tungsten surfaces, changes the condensation behavior of cadmium completely as compared to that observed on clean tungsten. Thermal accommodation of cadmium on oxygenated tungsten is incomplete on a small fraction of the surface.

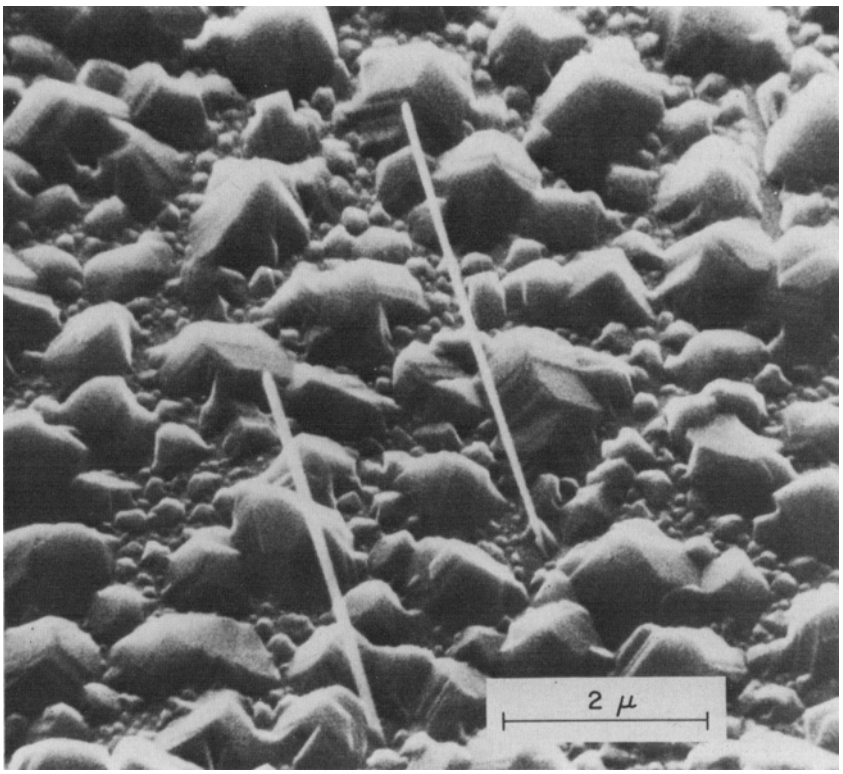

Fig. 16—Cadmium whiskers in the center of a tungsten grain. Scanning electron micrograph of deposit of 500 monolayers average thickness; see subscript Fig. 12.

The capacity of the tungsten surface for chemisorption of cadmium is greatly reduced by oxygen, and the heat of adsorption is diminished from 27 to 51 kcal per g-atom to 18.5 kcal per g-atom. The surface oxygen constitues a nucleation barrier, the effects of which are evident in the morphology and orientation of the cadmium deposit. Islands of irregular orientation are formed, reflecting little, if any, influence of the orientation of the underlying tungsten grain. The highly polycrystalline deposit shows a high evaporation coefficient, $\beta = 0.90$. In contrast, cadmium deposits on clean tungsten are epitaxial and show a rather low evaporation coefficient, $\beta = 0.63$.

The kinetic study of the early stages of growth shows a high adatom concentration (4×10^{14} cm^{-2}) at the critical nucleation. This indicates that only part of the adatoms are involved in the statistical density fluctuations leading to nucleation. The desorption flux from the adlayer can be used to monitor the thermodynamic potential of cadmium in the layer up to the point of nucleation. This gives a rather direct equilibrium measurement of the critical supersaturation. The fact that this leads to the same results as more conventional measurements shows that the nucleation problem could be treated as an equilibrium problem, as has indeed been done.

Beyond the critical point, monitoring of the thermodynamic potential of the nucleated deposit shows that it remains quite high compared with that of bulk crystalline cadmium. This indicates that the Ostwald ripening of the deposit is a slow process on the timescale of these measurements (10 min).

Comparison of the nucleation data with heterogeneous nucleation theory shows the theory to be inadequate for a quantitative description. The phase transformation theory advanced by Fowler and Guggenheim comes closest, but improved expressions for the entropy of atoms in the critical adlayer are needed. Furthermore, neither theory provides adequate expressions for the energy of interaction as a function of cluster size.

In summary we conclude the following:

1) Contaminants which adsorb strongly on the substrate surface have a very strong influence on the nucleation barrier and on the morphology of metal deposits. This emphasizes the importance of performing nucleation experiments under clean ultrahigh vacuum conditions.

2) The heat of adsorption of cadmium on oxygenated tungsten is 18.5 ± 1 kcal per g-atom for monomers. Bulk cadmium islands nucleate at a coverage of about 0.5 monolayer (4×10^{14} cm^{-2}). They have almost random orientation and eventually form a polycrystalline deposit with an evaporation coefficient $\beta = 0.90$.

3) The present experimental approach makes it possible to measure the equilibrium thermodynamic potential, the adatom concentration, and the heat of adsorption during deposition.

4) The critical nucleation stage of deposition can be described by an equilibrium thermodynamic potential which can be obtained experimentally.

5) Present nucleation theory is inadequate to account quantitatively for the experimental results. In view of (4) it is expected that an equilibrium treatment of the problem is the more likely to be successful.

ACKNOWLEDGMENTS

We thank Miss S. E. Koonce for the electron diffraction identification of cadmium whiskers, G. W. Kammlott for the scanning electron micrographs, C. J. Doherty for experimental assistance, and K. A. Jackson for helpful discussions.

REFERENCES

1. A. C. Zettlemoyer. ed.: *Nucleation,* Marcel Dekker, New York, 1969.
2. J. P. Hirth and G. M. Pound: *Condensation and Evaporation,* MacMillan, New York, 1963.
3. R. S. Wagner and R. J. H. Voorhoeve: *J. Appl. Phys.*, in press.
4. H. Shelton and A. Y. Cho: *J. Appl. Phys.*, 1966, vol. 37, pp. 3544-48.
5. A. Y. Cho and C. D. Hendricks: *J. Appl. Phys.*, 1969, vol. 40, pp. 3339-45.
6. J. B. Hudson and J. S. Sandejas: *Surface Sci.*, 1969, vol. 15, pp. 27-36.
7. J. B. Hudson: *J. Vac. Sci. Technol.*, 1970, vol. 7, pp. 53-61.
8. J. A. Becker, E. J. Becker, and R. G. Brandes: *J. Appl. Phys.*, 1961, vol. 32, pp. 411-23.
9. B. McCarrol: *J. Chem. Phys.*, 1967, vol. 46, pp. 863-69.
10. A. N. Nesmeyanov: *Vapor Pressure of the Elements,* J. I. Carasso, ed., pp. 202-452, Academic Press, New York, 1963.
11. V. J. Mimeault and R. S. Hansen: *J. Chem. Phys.*, 1966, vol. 45, pp. 2240-50.
12. P. W. Tamm and L. D. Schmidt: *J. Chem. Phys.*, 1969, vol. 51, pp. 5352-63.
13. R. A. Collins and B. H. Blott: *J. Appl. Phys.*, 1969, vol. 40, pp. 5390-91.
14. T. L. Cottrell: *The Strengths of Chemical Bonds,* p. 272, Butterworths, London, 1958.
15. C. C. Chang: Ph.D. Thesis, Cornell University, 1967.
16. J. C. Tracy and J. M. Blakely: *Surface Sci.*, 1969, vol. 15, pp. 257-76.
17. Yu. G. Ptushinskii and B. A. Chuikov: *Surface Sci.*, 1967, vol. 6, pp. 42-56; *Surface Sci.*, 1967, vol. 7, pp. 90-92.
18. C. Kohrt and R. Gomer: *J. Chem. Phys.*, 1970, vol. 52, pp. 3283-94.
19. F. D. Rossini, D. D. Wagman, W. H. Evans, S. Levine, and I. Jaffe: *Selected Values of Chemical Thermodynamic Properties,* Circ. 500, *Nat. Bur. Stand.*, Washington, 1952.
20. G. Herzberg: *Spectra of Diatomic Molecules,* pp. 395, 516, Van Nostrand, Princeton, N.J., 1950.
21. H. Kuhn and S. Arrhenius: *Z. Physik,* 1933, vol. 82, pp. 716-22.
22. G. Wessel: *Z. Physik,* 1951, vol. 130, pp. 539-48.
23. M. Volmer: *Kinetik der Phasenbildung,* p. 103, Steinkopff Verlag, Dresden, 1939.
24. B. K. Chakraverty and G. M. Pound: in *Condensation and Evaporation of Solids,* E. Rutner, P. Goldfinger, and J. P. Hirth, eds., pp. 553-65, Gordon and Breach, New York, 1964.
25. W. C. Ellis, D. F. Gibbons, and R. G. Treuting: in *Growth and Perfection of Crystals,* R. H. Doremus, B. W. Roberts, and D. Turnbull, eds., pp. 102-18, John Wiley & Sons, New York, 1958.
26. R. S. Wagner and W. C. Ellis: *Trans. TMS-AIME,* 1965, vol. 233, pp. 1053-64.
27. J. Frenkel: *Z. Physik,* 1924, vol. 26, pp. 117-38.
28. J. W. Gibbs: *The Scientific Papers, vol. 1, Thermodynamics,* p. 258ff., Dover Publications, New York, New York, 1961.
29. M. Volmer and A. Weber: *Z. Physik. Chem.*, 1926, vol. 119, pp. 277-301.
30. M. Volmer: *Kinetik der Phasenbildung,* p. 121, Steinkopff Verlag, Dresden, 1939.
31. R. H. Fowler and E. A. Guggenheim: *Statistical Thermodynamics,* p. 432, University Press, Cambridge, 1965.
32. K. L. Moazed and G. M. Pound: *Trans. TMS-AIME,* 1964, vol. 230, pp. 234-39.
33. R. D. Gretz and G. M. Pound: in *Condensation and Evaporation of Solids,* E. Rutner, P. Goldfinger, and J. P. Hirth, eds., pp. 575-97, Gordon and Breach, New York, 1964.
34. R. H. Fowler and E. A. Guggenheim: *Statistical Thermodynamics,* pp. 429-37, University Press, Cambridge, 1965.
35. D. Walton: in *Nucleaton,* A. C. Zettlemoyer, ed., pp. 379-404, Marcel Dekker, New York, 1969.
36. R. Becker and W. Döring: *Ann. Phys.*, 1935, vol. 24, Series 5, pp. 719-52.
37. G. M. Pound, M. T. Simnad, and L. Yang: *J. Chem. Phys.*, 1954, vol. 22, pp. 1215-19.
38. J. D. Cockcroft: *Proc. Roy. Soc., A,* 1928, vol. 119, pp. 293-312.
39. T. L. Cottrell: *The Strengths of Chemical Bonds,* p. 270 ff, Butterworths, London, 1958.
40. G. M. Martynkevich: *Russ. J. Phys. Chem.*, 1970, vol. 44, pp. 182-85.
41. J. P. Hirth and G. M. Pound: *Condensation and Evaporation*, pp. 41-44, MacMillan, New York, 1963.
42. V. K. Semenchenko: *Surface Phenomena in Metals and Alloys,* pp. 88, 404, Pergamon Press, New York, 1961.